Sarrus Linkage Aerial Drone Arm

Jacob Lemirick
Department of Mechanical Engineering Idaho State University
Pocatello, ID, USA
jacoblemrick@isu.edu

Wesley Thomas
Department of Mechanical Engineering
Idaho State University
Pocatello, ID, USA
thomwesl@isu.edu

Parker Wegrowski
Department of Mechanical Engineering Idaho State University
Pocatello, ID, USA
parkerwegrowski@isu.edu

Taher Deemyad
Department of Mechanical Engineering Idaho State University
Pocatello, ID, USA
deemtahe@isu.edu

***Abstract*— The final goal of this project is to design an advanced robotic sampling mechanism that can be deployed by an unmanned aerial vehicle (UAV) to obtain small objects. The focus of this part of the research is only on designing the lightweight, foldable robotic arm for this system. The arm will be designed to utilize Sarrus linkages to efficiently retract and extend. This arm has one degree of freedom and the motion in this arm can be controlled by torsional springs and one actuator. In the final design, the arm, initially, will be in the retracted position, which will allow it to be stored in a streamlined case to minimize interference with the objects in the path of the drone as it flies. Once the drone has reached the desired location, the arm will extend to its full length to reach the target object. In this paper, a foldable arm has been completely analyzed, designed in SolidWorks, and a prototype of it was built and successfully tested. In the next stage of this project, a novel gripper would be designed for this mechanism.**

Keywords*— *Single Motor, Minimum Actuation, Foldable Mechanisms, Robotic Arm, Drone, UAV, UGV, Quadcopter, One Degree of Freedom, Sarrus linkage.

I. Introduction

When considering advances in the technology of unmanned and autonomous systems in the modern age, using drones comes to the center of attention. With the potential to be specially designed for complex tasks and harsh environments that are either too dangerous or too ill-suited for humans, drones are at the forefront of exploration and innovation, while simplifying tasks such as delivery and transportation. Having manipulators and detection systems for ground vehicles is very common [15], [16] while it is not that common in UAVs. A key step towards expanding the capabilities of drones is producing systems to allow a drone to grasp and manipulate objects. Coupling a manipulator with an unmanned aerial vehicle – with the ability to pass obstacles and rough terrain which is too difficult for either humans or autonomous ground vehicles – is of particular interest [13], [14].

Some simple grippers can be designed that are actuated by tendons. Such a gripper can be easily connected or even incorporated inside of the body of drones. Alternatively, a very lightweight, cylindrical net can be affixed to the bottom of the drone. By leaving the bottom of the net open, and actuating it via the use of twisting ropes, it can be made to constrict around objects [10]. While these systems are useful and lightweight, such designs without an extendable robotic arm are limited in their utility. For instance, they cannot acquire objects that are positioned under another object (such as fruits hanging underneath the tree).

A resembled human arm and hand design with a shoulder, upper arm, elbow, lower arm, wrist, and hand is both familiar (aiding human operators) and flexible (allowing for complex operations) [1]. By adding multiple such arms, the capability and flexibility of the drone can be greatly increased [2]. Such designs have near omnidirectional mobility, the ability to grasp objects of considerable size and perform tasks beyond traditional manipulators. In a similar design, the manipulators are removed, and instead, a pair of arms are used to grasp objects. Such a design offers similar flexibility to a humanoid arm but does not require a complex manipulator with a set of actuators [3], [4]. However, such a design is not ideal for every application. For simple tasks, flexibility does not add anything, similar to how the human arm is unnecessary for an autonomous system, and the excess actuators and joints, considerably increase the weight of the drone.

Using foldable three-dimensional linkages potentially offers the required degree of freedom to the robotic arm for most of the tasks, while the required space will be reduced. By arranging a "cage" of folding rods between two baseplates, the lower plate can be moved in virtually any direction by actuating the connections to the upper plate [5]. This style of design can overcome one of the challenges of creating an aerial manipulator: stability [6]. However, such a design still requires multiple actuators to operate each rod and like the humanoid arm, still offers more flexibility than is required for simple tasks.

More complex linkages, possessing two separately moving but related appendages, can incorporate a counterbalance system [9]. This kind of arm addresses one of the major hurdles for UAV manipulators. Unlike terrestrial vehicles, aerial vehicles operate in an unstable environment and they must be able to support the whole weight of the system and maintain their orientation. Using such a mechanism can be a good option, which increases the stability of the system in exchange for increasing the weight of the arm. Alternatively, by reducing the total weight of the arm, the size of the arm can be maintained, while still reducing the overall effect of the arm on the center of gravity and balance.

Two-dimensional linkages plus the motions from drones allow for using fewer actuators for doing tasks. A design utilizing a five-bar linkage and three actuators to rotate the arm about the body of the drone and using the motion of the drone to compensate for what freedom is lost, allows this manipulator to do its tasks with fewer actuators [7]. By relying more on the motion from drones, it is possible to eliminate more actuators.

Using tension, it is possible to produce a unique gripping mechanism that utilizes only one actuator. A "finger" that is flexible on one side, but rigid on the other, can be forced to bend by applying tension to a cable attached to the flexible

This work supported by Idaho State Board of Education (SBOE) Grant for STEM

side. If the gripper is made of multiple fingers, the fingers can wrap around the target object and it can act as a form-closed grasper [8]. This manipulator utilizes minimal actuation; instead of relying on heavy actuators, such a design utilizes alternative sources of force – in this case, gravity –to move.

II. Mechanism Components and Material

A. Components

The base element of this arm is a Sarrus linkage. Each linkage consists of four hinged sides, comprised of two plates, and connected to central main plates by revolute joints. The central joint between the side plates is operated by a torsional spring, set to hold the hinge in the open or extended position. The ends of the linkages match one another, allowing the end of one linkage to be the start of the next linkage. All main plates possess a central hole, except the end main plate, which possesses an anchor point. The first plate is connected to a rotating pulley, to be driven by a rotary actuator. A cable, coiled around the pulley, passes through the central holes and is secured to the anchor point on the final main plate. The main parts of this mechanism are shown in Fig. 1 and Table 1.

TABLE I. Component List

Part Number	Part	Quantity
1	Motor Main Plate	1
2	Main Plate	1
3	End Main Plate	1
4	Tether	1
5	Drum	1
6	Side Plate	16
7	Pin	20
8	Pin Nut	20
9	Spring	8

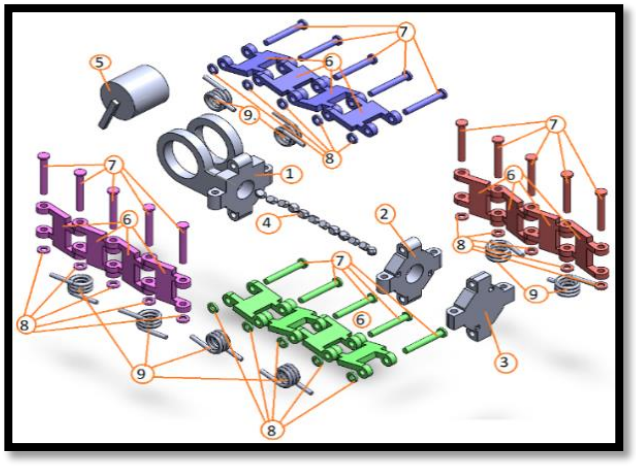

Fig 1. Component view

B. Material

The prototype of this arm has been made of Acrylonitrile Butadiene Styrene (ABS) plastic, and a pliable rubber-coated wire, serving as the central cable. Overall, this prototype weighs roughly 450g (0.45 kg). Based on the primary consideration for minimization of the weight of the arm, and selecting material with low density and high strength, ABS is an appropriate choice. While the weight of the intended payload for the mechanism is minor, the structure needs to be able to support the payload and its own weight at its maximum extension. ABS possesses a yield strength between 13 and 65 MPa, with a density of 1003 to 1193 kg/m^3. Low-grade aluminum alloys are a possible alternative. For example, aluminum 3003, has a density of 2733 kg/m^3, but offsets the increase in weight with greater strength; having a tensile yield strength of 124 MPa. Other types of plastic, such as Nylon 6 with a density of 1072 to 1297 kg/m^3 and a tensile yield strength ranging from 34 to 186 MPa, are also viable options.

III. Kinematics Analysis

A. Motion Analysis

Without any force applied to the pulley, the torsional springs force the hinged sides of each Sarrus linkage into their open or extended position. Fig. 2 is related to this arm in the open and fully extended position. By actuating the pulley, the cable can be spooled around the pulley, applying force to the final plate, and pulling it towards the first plate. As the final plate moves towards the first plate, the springs are compressed, closing the hinges, and bringing the entire structure into its collapsed position. When the cable is allowed to unspool again, the springs return to their rest positions, causing the arm to unfold into its extended position. Fig. 3 shows the complete motion of this mechanism from fully extended to completely collapsed positions.

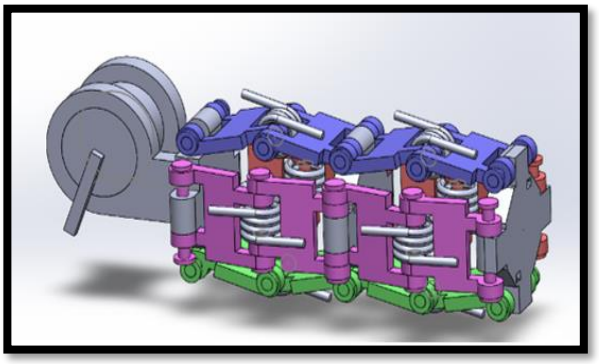

Fig 2. Foldable arm with Sarrus linkages in the fully extended position

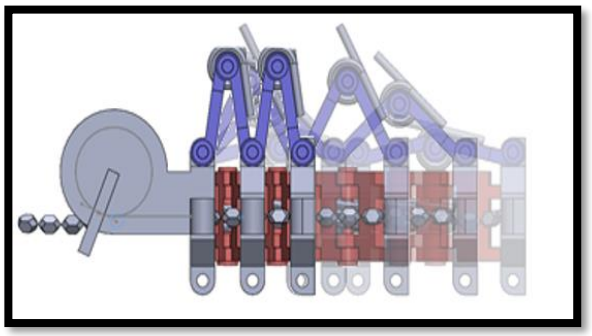

Fig 3. The motion of the foldable arm with Sarrus linkages from fully extended to collapsed positions

When the arm is collapsed, extended length is converted to perpendicular width. The relationships for an optimized arm (with main plates designed to rest face on the face when fully collapsed) between collapsed width, extended length and collapsed length are described by (1) through (3).

$$W = 2L_1 + L_2 \quad (1)$$

$$Extended\ Length \cong 2(N_b - 1) \times (L_1) \quad (2)$$

$$Collapsed\ Length \cong N_b \times t_b \cong (N_b - 1) \times 2t_s \quad (3)$$

$$W = Collapsed\ Width$$

$$L_1 = Side\ Plate\ Length$$

$$L_2 = main\ Plate\ Length$$

$$N_b = Number\ of\ Base\ Plates$$

$$t_b = thickness\ of\ Base\ Plates$$

$$t_s = thickness\ of\ side\ Plates$$

The extended length can be increased either by increasing the length of the side plates (which will increase the width of the collapsed arm) or by increasing the number of segments (which will increase the length of the collapsed arm). A prototype of this mechanism with a side plate length of 2.5 cm, the main plate thickness of 0.85 cm, and a width of 3.8 cm, can be fit in an 8.9 cm×8.9 cm×5 cm box. This mechanism can be extended for a maximum extension of 20.5 cm.

B. Mobility and Force Analysis

As it was mentioned, this arm is made of several Sarrus linkages. Because of the similarity between these linkages, mobility analysis for one of them would apply to the whole system. Fig. 4 shows the kinematic sketch for one Sarrus linkage in this arm. The links in this figure are shown with integer numbers while the joints are tagged with Roman numbers. Each Sarrus linkage consists of two main plates which are connected by eight side plates (two plates on each side) from four sides. According to this figure, each Sarrus linkage is made of 10 links and 12 revolute joints. This kinematic sketch is only a schematic model for mobility calculation purposes and the size and position of links are not on an accurate scale.

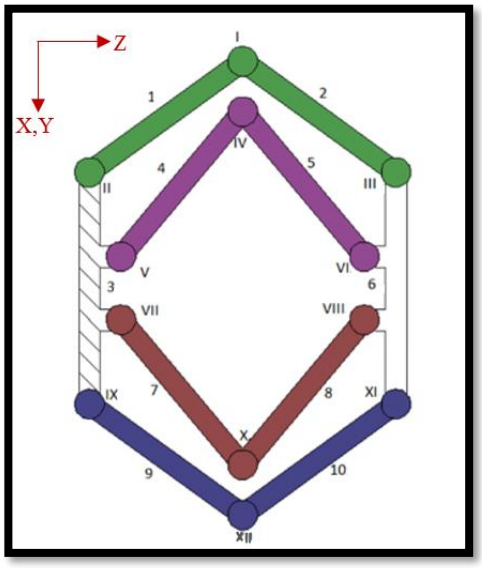

Fig 4. Kinematic sketch of a Sarrus linkage with four sides (a 3D mechanism which is shown in 2D)

This mechanism is a 3-dimensional structure that moves in space. Equation (4) is the Chebychev–Grübler–Kutzbach (K.G.C) equation which is also called the mobility equation (spatial case) and can be used for finding the mobility of this mechanism.

$$D.O.F. = 6(L - 1) - \sum_{i=1}^{J}(6 - fi) \quad (4)$$

$$L = Number\ of\ links$$
$$J = Number\ of\ joints$$
$$f_i = degree\ of\ freedom\ for\ each\ joint$$

Based on (4) and the following information the mobility of the Sarrus linkage has been calculated in (5).

$$L = 10\,, \quad J = 12\,, \quad f_i = 1$$
$$D.O.F. = (6 \times 9) - (12 \times 5) = -6 \quad (5)$$

However, in reality, this system is not an over-constrained mechanism (a negative degree of freedom). Because of symmetry in the Sarrus linkage, one set of links from each side can be removed (keep two perpendicular sets of links). In other words, because two sides of Sarrus linkage (purple-brown) in Fig. 4 are completely symmetric with the other two sides of linkage (blue-green), one of the pair from each side can be removed from the mechanism (for better understanding, look at the links with similar color in Fig. 2 and Fig. 4). Fig. 5 presents the kinematic sketch of the mechanism after removing the corresponding extra links (Blue links from one side and pink links from other side are removed).

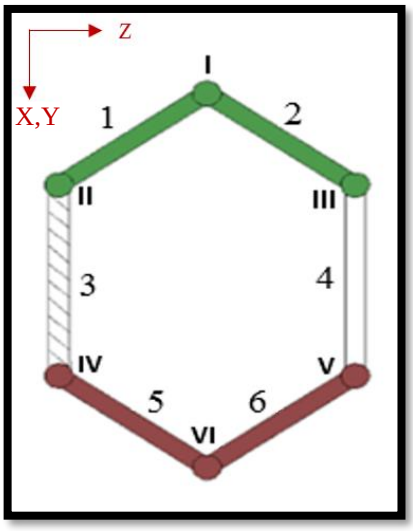

Fig 5. Kinematic sketch of Sarrus linkage without symmetric links

The motion of this mechanism is still a spatial case because we have two perpendicular sets of links. Note that in this simplification for Sarrus linkages, we cannot keep two parallel sets of links (that will increase the required degree of freedom). For this simplified model, the degree of freedom has been calculated in equation (6).

$$L = 6\,, \quad J = 6\,, \quad f_i = 1$$
$$D.O.F. = (6 \times 5) - (6 \times 5) = 0 \quad (6)$$

As it can be seen, the mobility of the system is reduced to 0 but still, it is over-constrained. In Fig. 5, the mechanism has two similar motions, one in the x-z plane and one in the y-z plane. Because the links are completely identical and the links made a 90-degree angle with each other, this is a unique case

that with some changes can be shown as a planar case. To solve this issue this mechanism can be simplified to the one shown in Fig. 6. In this case, the links on one side can be replaced by a prismatic joint (slider) to reflect how this mechanism operates in the plane.

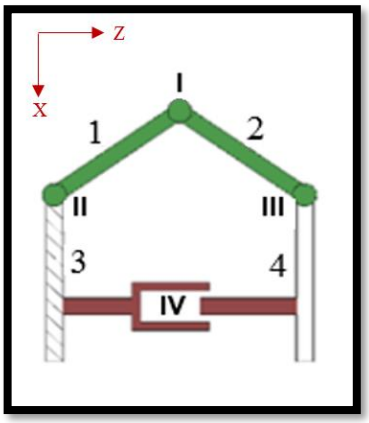

Fig 6. Kinematic sketch of simplified Sarrus linkage

Equation (7) shows the mobility for the planar case. Based on the number of joints and links in the simplified model (Fig. 6), and using the K.G.C equation for the planar case, the final mobility of a Sarrus linkage is found in (8) which is equal to 1. Given the mechanism aligns all Sarrus Linkages along the same axis, it maintains a single degree of freedom, and needs one actuator to move and perform tasks.

$$D.O.F. = 3(L-1) - \sum_{i=1}^{J}(3-fi) \quad (6)$$

$$L = Number\ of\ links$$
$$J = Number\ of\ joints$$
$$f_i = degree\ of\ freedom\ for\ each\ joint$$

$$L = 4\ , \quad J = 4\ , \quad f_i = 1$$

$$D.O.F. = (3 \times 3) - (4 \times 2) = 1 \quad (8)$$

The amount of force required to compress the arm is a function of the equivalent spring constant of all the springs in this mechanism. The springs are located between the side plates in this mechanism with each Sarrus linkage including up to four identical springs acting in parallel while the Sarrus linkages act in series with each other. The equivalent spring constant for this mechanism can be calculated from Equation (9).

$$k_{total} = \frac{(N_S \times k)}{N_L} \quad (9)$$

$$N_L = Number\ of\ sarrus\ linkage$$
$$N_S = Number\ of\ springs\ per\ linkage$$
$$k = Spring\ constant$$

To have a similar extension/collapse between the Sarrus linkages in mechanism during motion, the force between each linkage has to be balanced in the whole structure. Therefore, each Sarrus linkage have to have same number of springs with a similar constant coefficient, and therefore, the equivalent spring constant for each Sarrus linkage would be the same and the distance each linkage collapses will be equal too.

IV. Prototype

After motion analysis and simulation in SolidWorks, a prototype of this arm was constructed from ABS to test the functionality of the design. The design for the prototype follows a slightly altered pattern. This new pattern was used to accommodate the current springs and was in an attempt to ensure the strength of the joints during testing. However, these changes did not enough improve the performance of the mechanism. To provide the required force to extend the arm, torsion springs were used on the hinges. However, these springs did not span the full angle necessary to move the arm to full extension. At maximum length, the prototype could reach roughly 33 cm from the center of the first main plate to the center of the final main plate. In the collapsed position, the size of the arm is roughly 10.2 cm, meaning the entire arm has an extension ratio of a little over 3 to 1. The arm's operation proved controllable via rotating the pulley located on the first main plate. The motion of this prototype between fully extended to completely collapsed position is shown in Fig. 7.

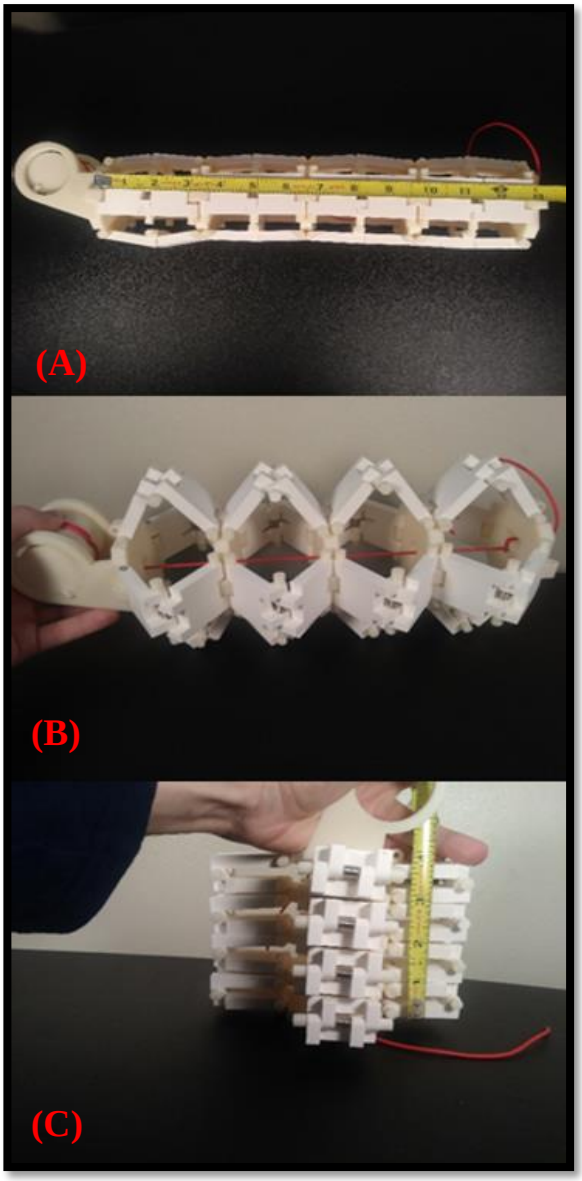

Fig 7. The motion of the prototype of the arm A) fully extended B) middle of motion C) completely collapsed

V. Results and Discussion

This mechanism has been designed based on two parameters: minimum required space and minimum weight. These parameters are critical for designing robotic arms for UAVs. The ratio between the minimum and maximum height of the arm is the key trait for efficient use of space. In this mechanism which includes four Sarrus linkages, this ratio is more than 3 which is acceptable. On the other hand, one of the main sources of weight in robotic arms is the actuation system. To minimize the total weight of the arm, this mechanism was designed to be able to operate with a minimum number of actuators. As has been shown the Sarrus linkage has one D.O.F. and requires only one actuator to move.

The arm demonstrated an expected behavior. In general and based on design requirements, this arm can satisfy the aims of this project. This arm, because of the presence of torsional springs between the side plates, initially was in a stretched state. The arm operated with one degree of freedom, which was controllable via the rotation of the pulley. Each linkage compressed an equivalent amount as the arm collapsed. Because of using springs with a high constant value, in this prototype, each linkage is operated by only two springs. To switch the state of the arm from stretched to a collapsed position, an external force is required. According to the degree of freedom of the mechanism, this arm can operate with a single servo motor that is connected to a pulley-cable system. One end of the cable is connected to the end main plate and the other end of it is connected to the pulley. When the pulley rotates, the cable will be wrapped around the pulley and the force from the cable will overcome the force of the springs, forcing the arm to collapse. Another considerable advantage of this design is the control over the amount of the extension of the arm. Due to each Sarrus linkage being operated by only two springs, the equivalent spring force can be found from (10).

$$k_{total} = \frac{(N_S \times k)}{N_L} = \frac{2k}{4} = 0.5k \qquad (10)$$

After simulation analysis in SolidWorks, in the actual tests of the prototype, the pulley was released properly and the arm extended to the rest position in response to the force applied by the springs. Although the prototype of the arm performed well in the actual tests, some changes can be made to this design to improve the performance of the system.

First of all, the springs have to be changed. The current springs have a rest angle of roughly 90 degrees while the hinges between the side plates have to be able to rotate to about 180 degrees to reach the fully extended position. Also, the used springs are with a high spring constant, if they are replaced by softer springs with a lower constant value, controlling the arm would be easier to collapse. In addition, because of a high spring constant, the springs have been used only on two sides of the Sarrus linkages. Utilizing softer springs on all four sides would result in much smoother motion. Even with only using these springs in half of the linkages, the arm still returns very quickly to the rest position, the pulley requires significant torque to pull the arm closed, and the pins are under significant stress. In the final design, using the softer springs with a complete range of motion for the side plates (a little less than 180 degrees) would be preferable. The maximum range of motion for the hinges has to be less than 180 degrees because this is one of the mechanical singularity positions and must be avoided [11], [12]. This position is shown in Fig. 8.

Second, the design can be optimized to reduce weight and better resist stress. This prototype is designed only to demonstrate the mobility and proof of operation of the arm. During the test of this prototype, it was observed that some parts of the arm were over-reinforced while some others were weak. The side and main plates with thicknesses of 0.81 cm and 0.89 cm respectively, demonstrated no signs of bending or stress. In contrast, each pin – sized to fit the springs – had a diameter equal to 0.33 cm and had less strength than the rest of the mechanism. Bending in the pins could often be observed when the arm was fully collapsed. Over time, after a few dozen complete motion tests, several pins failed and needed to be replaced! By optimizing each piece based on weight and the stresses, it experiences, an arm with minimum weight and higher strength can be designed. An alternative solution would be to use other materials like various Aluminum alloys in different parts of the mechanism.

Third, in addition to optimizing for weight and stress, the design can be optimized for better efficiency. Each side plate was hinged to allow the arms of the spring to maintain constant contact with them throughout opening and closing. However, this necessitated the hinges being offset from the edge of the side plates, resulting in significant extra space between the side plates in the closed position.

In addition, in the current design, each connection between the main plate and side plate has been secured by a separate pin. Each main plate (excepting the end-plates) is connected to two side plates from the sides, and therefore, it needs two pins per side. As such, the effective thickness of the main plates was greater than what was structurally necessary. In this situation, the collapsed length is described by (11).

$$Collapsed\ Length = (N_b - 1) \times ((2 \times t_s) + t_b) \qquad (11)$$

$$N_b = Number\ of\ Base\ Plates$$

$$t_s = thickness\ of\ side\ Plates$$

$$t_b = thickness\ of\ base\ Plates$$

If a single pin is used to connect two side plates to the main plate, then t_b will be equal to zero, and the equation (11) simplifies to equation (3). Utilizing a single pin at the connection between the main plates to the side plate, coupled with designing the side plates to incorporate the arms of the springs will result in extra space between the plates in the collapsed position being removed. In this situation, the main plates will be in contact with one another. These two changes will allow the arm to collapse with a minimum required length.

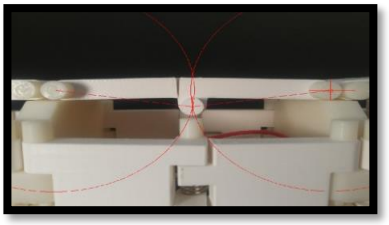

Fig 8. Singularity in the Sarrus linkage, caused by the central pin being offset from the side plates. Maximum extension occurs when the red circles are tangent

In Fig. 8, the pattern of motion for mechanism and plates using a single pin between side and main plates, are shown with red dash lines and arcs.

The last possible improvement is related to singularities avoidance. The side plates can be shaped to prevent singularity positions. In the collapsed position, although the side plates are parallel to each other, the singularity will not happen because of the presence of the springs. However, a singularity can happen in the fully extended position. The maximum extension of the arm will happen when the three pins are in line with each other (two pins between side plates and top/bottom main plates and one pin between side plates). On the prototype, maximum extension occurred at roughly 157.6 degrees. However, the hinge can extend beyond 157.6 degrees; it is able to open to a full 180 degrees, which is a singularity position. Howbeit, on this prototype, due to insufficient range of applied force by the springs, at the point of maximum extension, this singularity occurred irregularly. If the springs are replaced by ones with a greater rest angle as previously mentioned then a singularity will occur whenever the hinges are allowed to extend beyond their equilibrium point. As such, each hinge will need to be optimized so that it cannot rotate beyond the point of maximum extension. Furthermore, at maximum extension, the arm exists in a position of unstable equilibrium. This is a potential singularity point as well if the forces acting on the arm act perfectly down the length of the arm. Although during testing the prototype, none of the hinges demonstrated a singularity due to unstable equilibrium, it is theoretically possible. Limiting the rotation of the hinge so that it is limited to an angle slightly less than maximum extension, would help to ensure that the pulley is reliably able to extend the arm. In the final design, all of these points will be considered in order to produce an optimized design.

VI. Conclusion

In this research, a foldable mechanism for using as the arm for UAVs was studied. Sarrus linkages allow for the creation of foldable structures that possess a single degree of freedom. By stacking multiple linkages end to end, it is possible to create a structure that can extend from a compact, short configuration, to one of considerable length. Due to the structure maintaining a single degree of freedom, it is possible to control the extension of the structure via a single actuator and spring forces. Such a structure has the potential to be used as a lightweight and efficient arm for autonomous aerial vehicles that focuses simultaneously on saving weight through the minimal use of actuators and optimizing. Such an arm would allow a UAV to perform simple but important tasks such as sampling, without requiring to carry some more complex and heavier arms. As such, operators could utilize smaller drones, or utilize larger drones with a minimal impact on flight characteristics. In this work, a simulation of this design was analyzed in SolidWorks, a prototype of this design was built and successfully tested. Finally, some suggestions for improvement of this design were presented.

References

[1] G. A. Yashin, D. Trinitatova, R. T. Agishev, R. Ibrahimov and D. Tsetserukou, "AeroVr: Virtual Reality-based Teleoperation with Tactile Feedback for Aerial Manipulation," 2019 19th International Conference on Advanced Robotics (ICAR), 2019, pp. 767-772, doi: 10.1109/ICAR46387.2019.8981574.

[2] Paul, H., Miyazaki, R., Ladig, R., & Shimonomura, K. (2020). Tams: Development of a multipurpose three-arm aerial manipulator system. Advanced Robotics, 35(1), 31–47. https://doi.org/10.1080/01691864.2020.1845237

[3] L. Kruse and J. Bradley, "A Hybrid, Actively Compliant Manipulator/Gripper for Aerial Manipulation with a Multicopter," 2018 IEEE International Symposium on Safety, Security, and Rescue Robotics (SSRR), 2018, pp. 1-8, doi: 10.1109/SSRR.2018.8468651.

[4] D. Kim and P. Y. Oh, "Toward Avatar-Drone: A Human-Embodied Drone for Aerial Manipulation," 2021 International Conference on Unmanned Aircraft Systems (ICUAS), 2021, pp. 567-574, doi: 10.1109/ICUAS51884.2021.9476704.

[5] D. Kim and P. Y. Oh, "Testing-and-Evaluation Platform for Haptics-based Aerial Manipulation with Drones," 2020 American Control Conference (ACC), 2020, pp. 1453-1458, doi: 10.23919/ACC45564.2020.9147799.

[6] P. Chermprayong, K. Zhang, F. Xiao and M. Kovac, "An Integrated Delta Manipulator for Aerial Repair: A New Aerial Robotic System," in IEEE Robotics & Automation Magazine, vol. 26, no. 1, pp. 54-66, March 2019, doi: 10.1109/MRA.2018.2888911.

[7] S. Hamaza and M. Kovac, "Omni-Drone: on the Design of a Novel Aerial Manipulator with Omni-directional Workspace," 2020 17th International Conference on Ubiquitous Robots (UR), 2020, pp. 153-158, doi: 10.1109/UR49135.2020.9144837.

[8] N. Iversen, O. B. Schofield and E. Ebeid, "LOCATOR - Lightweight and Low-Cost Autonomous Drone System for Overhead Cable Detection and Soft Grasping," 2020 IEEE International Symposium on Safety, Security, and Rescue Robotics (SSRR), 2020, pp. 205-212, doi: 10.1109/SSRR50563.2020.9292591.

[9] I. Abuzayed, A. R. Itani, A. Ahmed, M. Alkharaz, M. A. Jaradat and L. Romdhane, "Design of Lightweight Aerial Manipulator with a CoG Compensation Mechanism," 2020 Advances in Science and Engineering Technology International Conferences (ASET), 2020, pp. 1-5, doi: 10.1109/ASET48392.2020.9118288.

[10] L. Hingston, J. Mace, J. Buzzatto and M. Liarokapis, "Reconfigurable, Adaptive, Lightweight Grasping Mechanisms for Aerial Robotic Platforms," 2020 IEEE International Symposium on Safety, Security, and Rescue Robotics (SSRR), 2020, pp. 169-175, doi: 10.1109/SSRR50563.2020.9292581.

[11] Deemyad, T., Hassanzadeh, N. and Perez-Gracia, A., 2018, August. Coupling mechanisms for multi-fingered robotic hands with skew axes. In IFToMM Symposium on Mechanism Design for Robotics (pp. 344-352). Springer, Cham.

[12] Deemyad, T., Heidari, O. and Perez-Gracia, A., 2020, May. Singularity design for RRSS mechanisms. In USCToMM Symposium on Mechanical Systems and Robotics (pp. 287-297). Springer, Cham.

[13] Deemyad, T., Moeller, R. and Sebastian, A., 2020, October. Chassis design and analysis of an autonomous ground vehicle (AGV) using genetic algorithm. In 2020 Intermountain Engineering, Technology and Computing (IETC) (pp. 1-6). IEEE.

[14] Moeller, R., Deemyad, T. and Sebastian, A., 2020, October. Autonomous navigation of an agricultural robot using RTK GPS and Pixhawk. In 2020 Intermountain Engineering, Technology and Computing (IETC) (pp. 1-6). IEEE.

[15] Deemyad, T. and Sebastian, A., 2021, June. Mobile Manipulator and EOAT for In-Situ Infected Plant Removal. In IFToMM Symposium on Mechanism Design for Robotics (pp. 274-283). Springer, Cham.

[16] Deemyad, T. and Sebastain, A., 2021, September. HSL Color Space for Potato Plant Detection in the Field. In 2021 Fourth International Conference on Electrical, Computer and Communication Technologies (ICECCT) (pp. 1-8). IEEE.